Available online at www.sciencedirect.com
ScienceDirect
Journal of Photochemistry and Photobiology A: Chemistry 191 (2007) 59–65
Journal of Photochemistry and Photobiology A:Chemistry
www.elsevier.com/locate/jphotochem

Study on the binding of farrerol to human serum albumin

Jing Jin, Jingfeng Zhu *, Xiaojun Yao, Longmin Wu

State Key Laboratory of Applied Organic Chemistry, Lanzhou University, Lanzhou, Gansu 730000, China

Received 15 January 2007; received in revised form 16 March 2007; accepted 4 April 2007
Available online 7 April 2007

Abstract

Binding of farrerol to human serum albumin (HSA) was investigated at 293, 303, and 313 K and pH 7.40 using spectrophotometric technique and molecular modeling. The binding parameters obtained from the modified Scatchard's procedure were in close agreement with those from Stern–Volmer equation. Based on the thermodynamic parameters calculated from the van't Hoff equation, the enthalpy change ΔH° and entropy change ΔS° for the process of farrerol binding to HSA were evaluated at -18.51 kJ mol^{-1} and 47.52 J mol^{-1} K^{-1}, respectively. The value of 2.63 nm for the distance r between the donor (HSA) and acceptor (farrerol) was derived from the fluorescence resonance energy transfer. From these results, three issues on the interactions between farrerol and HSA could be approached: (a) farrerol is strongly bound to HSA, (b) the primary binding site is located at the site I of HSA, and (c) apart from hydrophobic interactions, there still exist hydrogen bond interactions between farrerol and the residues of HSA, such as Lys195, Arg218, Arg222, and Ala291. Besides, the conformational change of HSA was observed, being caused by the interaction with farrerol.

Keywords: Farrerol; Human serum albumin; Secondary structure; Spectrophotometric; Molecular modeling

1. Introduction

One of the important topics in pharmaceutical research is to learn the interaction of drug with proteins. Drugs can be incorporated into proteins which act as carriers. Among them human serum albumin (HSA) has been considered as a typical representative. HSA consists in blood plasma as a major protein component. Besides, it exists in interstitial fluids. HSA contributes to colloidal osmotic blood pressure and, most importantly, plays a key role in the transport of a wide variety of substances [1,2]. The X-ray crystallographic data for HSA reveal it actually to be a 585 amino acid residue monomer containing three homologous α-helical domains I, II, and III [3]. Each domain is constituted by two sub-domains A and B, which share common structural elements. In crystal these six sub-domains assemble to form a heart-shaped molecule [3]. Both of their aromatic and heterocyclic ligands are bound within two hydrophobic pockets in sub-domains IIA and IIIA, which are referred to as the sites I and II, respectively [2,4–5]. Seven binding sites are localized by fatty acids in sub-domains IB, IIIA, IIIB, and on the sub-domain interfaces [6]. HSA has also a high affinity-binding site to metal at the N-terminus [7]. The multiple binding sites underlie the exceptional ability of HSA to interact with many organic and inorganic molecules. Consequently, it becomes an important regulator of intercellular fluxes and displays a pharmacokinetic behavior in many drugs [8].

Otherwise, most of the flavonoid drugs show a high degree of binding to HSA, which is a primary determinant of their pharmacokinetic properties. The previous reports on these [8–11] involve quercetin, kaempferol, delphinidin, scutellarin, alpinetin, formononetin, etc. Farrerol (Scheme 1) is a new kind of 2,3-dihydro-flavonoid drug and has been synthesized as an antibechic. Investigations have shown that farrerol has a wide spectrum of physiological activities such as anti-inflammatory, anti-bacterial, and antioxidant activity for scavenging radicals and inhibiting a variety of enzymes [12]. Pathological experiments have demonstrated that farrerol relieves coughs and moves phlegm. It has been found that more than 95% of farrerols are primarily bound to HSA, which serves as a storehouse for farrerols, and the unbound moiety is pharmacologically active. Thus, the nature and magnitude of the interactions between farrerol and HSA have important pharmacokinetic and pharmacodynamic implications. Yet, few works have been published for

* Corresponding author. Tel.: +86 931 8912280; fax: +86 931 8625657.
E-mail addresses: jinjing@lzu.edu.cn (J. Jin), zhujingfeng1979@126.com (J. Zhu).

1010-6030/$ – see front matter © 2007 Elsevier B.V. All rights reserved.
doi:10.1016/j.jphotochem.2007.04.004

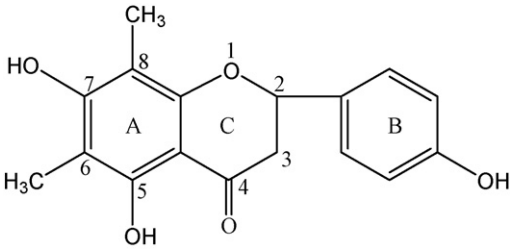

Scheme 1. The structure of farrerol.

the mechanism of the interactions and detailed physicochemical characterizations of farrerol binding to HSA.

Spectrophotometric techniques and molecular modeling studies have been widely used for monitoring drug binding to plasma albumin because of its sensitivity, accuracy, rapidity, and ease of use [13]. In the present paper, studies on the mechanism, mode, and conformation change of farrerol binding to HSA have been performed using spectroscopy and molecular modeling. The results have been discussed on the binding parameters, the identification of binding sites, the effect of farrerol on the conformation of HSA, and the nature of forces involved in the interactions.

2. Materials and methods

2.1. Materials

HSA fraction V was obtained from Sigma and essentially fatty acid free. Farrerol of analytical grade was obtained from National Institute for the Control of Pharmaceutical and Biological Products, China. All other reagents were of analytical grade. Double-distilled water was used throughout experiments. Solutions were prepared in 20 mM phosphate buffered saline (PBS) at pH 7.40, whose ion strengths were kept at 0.1 M. A 35 μM solution of HSA was prepared in a pH 7.40 PBS. A 0.3 mM methanol solution of farrerol was used for all the binding experiments. The concentration of HSA was determined spectrophotometrically on a Shimadzu UV-260 UV–vis spectrophotometer using ε_{280} (HSA) = 36,500 M^{-1} cm^{-1} [8].

2.2. Absorption spectra

UV–vis absorption was measured on a Shimadzu UV-260 UV–vis spectrophotometer in a 1 cm cuvette. The UV–vis spectra were scanned in the range of 240–300 nm and 300–500 nm at room temperature.

2.3. Fluorescence spectra

Fluorescence spectra were recorded on a PE LS55 fluorimeter in a 1 cm quartz cell following an excitation wavelength of 295 nm at a definite temperature over a wavelength range of 300–500 nm. The selection of 295 nm for excitation was to ensure the light absorbed by the tryptophan residue alone. The excitation and emission slits were 10 nm. Quantitative analysis of the interaction between HSA and farrerol was performed with a fluorimetric titration experiment as follows: 3 mL of a 3.5 μM solution of HSA was titrated by successive addition of farrerol solution to reach a final concentration of 6 μM farrerol. Spectrophotometric analysis of the fluorescence quenching was carried out with the Stern–Volmer equation (Eq. (1)) [14]:

$$\frac{F_0}{F} = 1 + K_{SV}[Q] = 1 + k_q\tau_0[Q] \quad (1)$$

where F_0 and F are the relative fluorescence intensities in the absence and presence of quencher, respectively, $[Q]$ the concentration of quencher, K_{SV} the Stern–Volmer quenching constant, k_q the quenching rate constant for a biomolecular reaction, and τ_0 is the average lifetime for fluorophore in the absence of quencher evaluated at 10^{-8} s [15]. Linear plots of F_0/F against $[Q]$ yield K_{SV} as slopes, and k_q can be calculated.

The binding parameters for the farrerol–HSA system have been derived from fluorescence quenching data inspected at 293, 303, and 313 K, respectively, according to the modified Scatchard's procedure (Eq. (2)) [16]:

$$\frac{F_0}{F} = K_A\left(\frac{[Q]F_0}{F_0 - F}\right) - nK_A[P] \quad (2)$$

where $[P]$ is the molar concentration of total HSA, $[Q]$ the molar concentration of total farrerol, n the binding stoichiometry per class of binding sites, and K_A the equilibrium binding constant.

The values for the enthalpy change (ΔH°) and entropy change (ΔS°) will be evaluated from the van't Hoff equation [17] by considering ΔH° not varying significantly over the experimental temperature range:

$$\ln K_A = -\frac{\Delta H^\circ}{RT} + \frac{\Delta S^\circ}{R} \quad (3)$$

where K_A is the binding constant at a definite temperature and R the gas constant. A linear plot of $\ln K_A$ against $1/T$ yields ΔH° and ΔS° for the binding interaction. Consequently, the amount of free energy change required for the binding is estimated from Eq. (4):

$$\Delta G^\circ = \Delta H^\circ - T\,\Delta S^\circ \quad (4)$$

2.4. Estimation of binding distance r

Eq. (5) defines E for the energy transfer efficiency based on the Förster's theory, where r is the distance from a ligand to a tryptophan residue of a protein, and R_0 the Förster critical distance, at which 50% of the excitation energy is transferred to an acceptor [18]. The value for r can be calculated from donor emission and acceptor absorption spectra according to the Förster formula (Eqs. (5)–(7)):

$$E = 1 - \frac{F}{F_0} = \frac{R_0^6}{R_0^6 + r^6} \quad (5)$$

$$R_0^6 = 8.8 \times 10^{-25} K^2 N^4 \Phi J \quad (6)$$

$$J = \frac{\int_0^\infty F(\lambda)\varepsilon(\lambda)\lambda^4\,d\lambda}{\int_0^\infty F(\lambda)\,d\lambda} \quad (7)$$

In Eq. (6), K^2 is the orientation factor related to the geometry of donor and acceptor, N the average refractive index of medium in the wavelength range where spectral overlap is significant, Φ the fluorescence quantum yield of donor, and J the spectral overlapping between the emission spectrum of donor and the absorption spectrum of acceptor (Fig. 7), which could be estimated from Eq. (7), where $F(\lambda)$ is the corrected fluorescence intensity of donor over a wavelength range of λ to $\lambda + \Delta\lambda$ and $\varepsilon(\lambda)$ the extinction coefficient of acceptor at λ.

2.5. Circular dichroism (CD) spectra

Circular dichroism spectral measurements were run on an Olis DSM 1000 automatic recording spectrophotometer in a 1 mm cell at 298 K. CD spectra were recorded over a wavelength range of 200–250 nm with a scan of 50 points. The concentration of HSA for CD studies was 3.5 μM. Ratios of HSA to farrerol were 1:1.70, 1:5.10, and 1:6.80, respectively. The spectrophotometric results were expressed as $[\theta]_{MRW}$ obtained from Eq. (8) [13]:

$$[\theta]_{MRW} = \frac{\theta_{Obs}\,(mdeg)}{cnl} \tag{8}$$

where $[\theta]_{MRW}$ represents the mean residue ellipticity, θ_{Obs} the measured ellipticity, c the molar concentration of HSA, n the number of amino acid residues, and l the optical path length. The α-helical contents of free and combined HSA were evaluated from $[\theta]_{MRW}$ at 210 nm based on Eq. (9) [13]:

$$\alpha\text{-helical}\,(\%) = \frac{-[\theta]_{MRW210} - 4000}{33,000 - 4000} \times 100 \tag{9}$$

2.6. Molecular modeling investigation

The crystal structure of HSA in the complex with R-warfarin was taken from the Brookhaven Protein Data Bank (entry codes 1h9z) [19]. The potential of the 3D structure of HSA was assigned to it as according to the Amber 4.0 force field with Kollman all atom charges. The initial structure of farrerol was given by molecular modeling software Sybyl 6.9 [20], whose geometry was subsequently optimized to reach the minimal energy using the Tripos force field with Gasteiger–Marsili charges. The replacement of R-warfarin in the HSA-warfarin crystal structure by the optimized structure of farrerol gave a structural model for the farrerol–HSA system. FlexX program was used to build farrerol–HSA interaction modes. All calculations were performed on a SGI O2 workstation.

3. Results and discussion

3.1. Interactions of farrerol with HSA and binding constants

The absorption spectra of HSA with various amounts of farrerol are shown in Fig. 1. The absorption of HSA is characterized by a weak band at 280 nm. Farrerol has no absorption bands in the range of 240–300 nm. The addition of farrerol (Fig. 1) led to a small increase in the HSA absorbance at 280 nm and a little red shift. These observations can be rationalized in terms of interactions between farrerol and HSA in the ground state and formation of a ground state complex. As it is known, dynamic collision only affects the excitation state of quenching molecules, whereas it has no influence on the absorption spectrum of quenching substances [21].

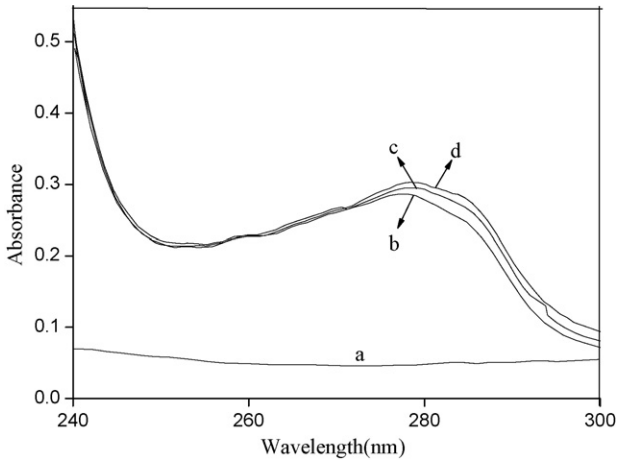

Fig. 1. Absorption spectra of: (a) a 9 μM farrerol solution, (b) a 7 μM HSA solution, (c) a 7 μM HSA solution containing 18 μM farrerol, and (d) a 7 μM HSA solution containing 36 μM farrerol.

Fig. 2 shows the fluorescence emission spectra of HSA with various amount of farrerol following an excitation at 295 nm. The emission of HSA is characterized by a broad emission band at 348 nm. Its intensity diminishing immediately followed the addition of farrerol. It implied that the molecule of HSA in the S_1 state was quenched by farrerol.

Fluorescence of HSA originates from tryptophan (Trp), tyrosine (Tyr), and phenylalanine (Phe) residues. Actually, the intrinsic fluorescence of HSA is mainly contributed by Trp alone, because Phe has a very low quantum yield and the fluorescence

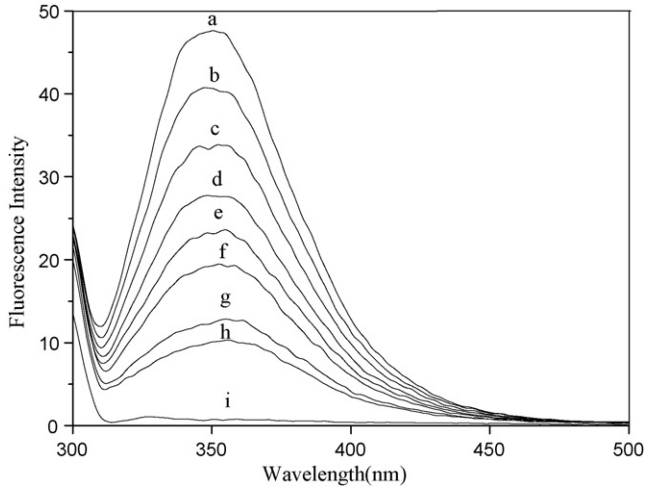

Fig. 2. Fluorescence spectra of HSA (3.5 μM) following the excitation at 295 nm, at pH 7.40 and 293 K. (a–h) Indicate the spectra recorded at [farrerol] = 0, 0.6, 1.2, 1.8, 2.4, 3.0, 4.8, and 6.0 μM, respectively and (i) indicates the spectrum recorded at [farrerol] = 3.0 μM.

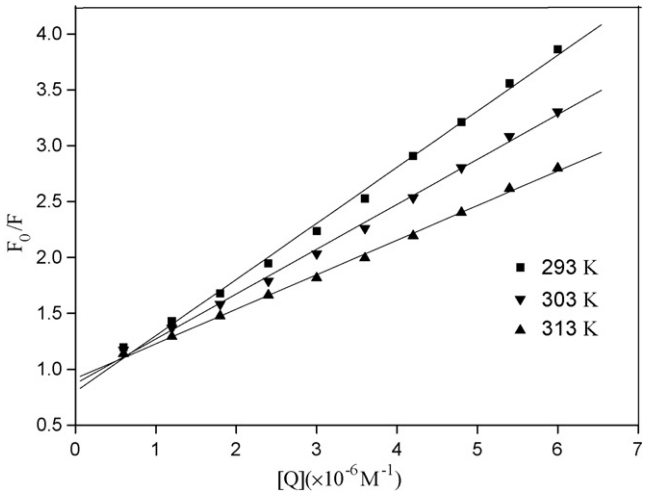

Fig. 3. Linear fits of fluorescence intensity change for the farrerol–HSA system to the Stern–Volmer equation at different temperatures.

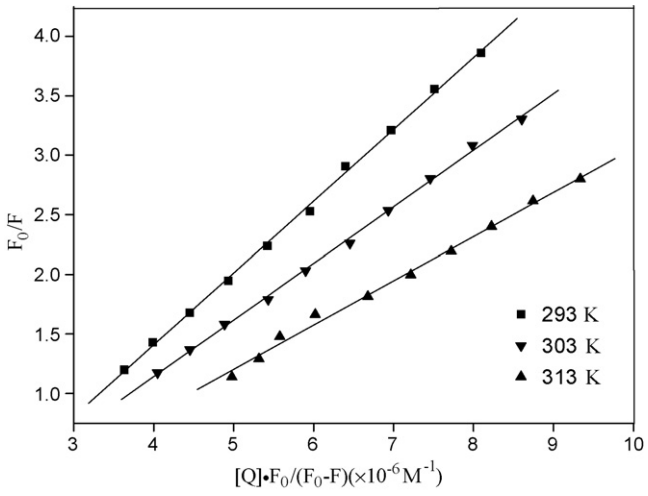

Fig. 4. Curve fits of fluorescence intensity change for the farrerol–HSA system to the modified Scatchard's procedure at different temperatures.

of Tyr is almost totally quenched when it is ionized or near by an amino group, a carboxyl group, or a Trp [22]. Therefore, the decrease in the intrinsic fluorescence intensity of HSA upon addition of farrerol implied that either the molecule of HSA experienced a quenching process or the microenvironment around Trp, i.e., Trp214, was changed [23]. A quenching process can be usually induced by a dynamic or a static quenching mechanism. Both mechanisms can be distinguished from each other by the differences in temperature-dependent behavior. Higher temperature leads to the dissociation of weakly bound complexes owing to a faster molecular diffusion. As a result, larger amounts of molecules are collisionally quenched and the quenching rate constant will increase with raising temperature. Such a process is termed a dynamic quenching process. In contrast to this, a static quenching process will lead to a decrease in the quenching rate constant with raising temperature. The static quenching was further confirmed from the values of quenching rate constant, k_q, which are evaluated using Eq. (1). The maximum scatter collision quenching constant, k_q, of various quenchers with the biopolymer is $2.0 \times 10^{10}\,M^{-1}\,s^{-1}$. If the quenching rate constant k_q for farrerol–HSA is greater than that of a scatter process. It may be attributed a quenching process initiated by drugs. So it shows that the quenching was not initiated by dynamic collision but forms compound, it was static quenching.

Spectrophotometric analysis of the emission change of HSA accompanying the variation in the concentration of farrerol was carried out with the Stern–Volmer equation (Fig. 3) and the modified Scatchard's procedure (Fig. 4), respectively, for which the Stern–Volmer quenching constant K_{SV} (Eq. (1)) and the equilibrium binding constant K_A (Eq. (2)) are derived, respectively. Their values are collected in Table 1. Values at each temperature derived from both theories seem to be fairly consistent with each other. The perfect linear correlations in Fig. 4 establish that farrerol binds to HSA at one kind of site, most likely binding to the site I in a hydrophobic pocket. This implication is supported by the very closed values for n (Table 1). The temperature feature of the binding constants, decreasing with raising temperature, and the k_q (Table 1) values of HSA quenching procedure initiated by

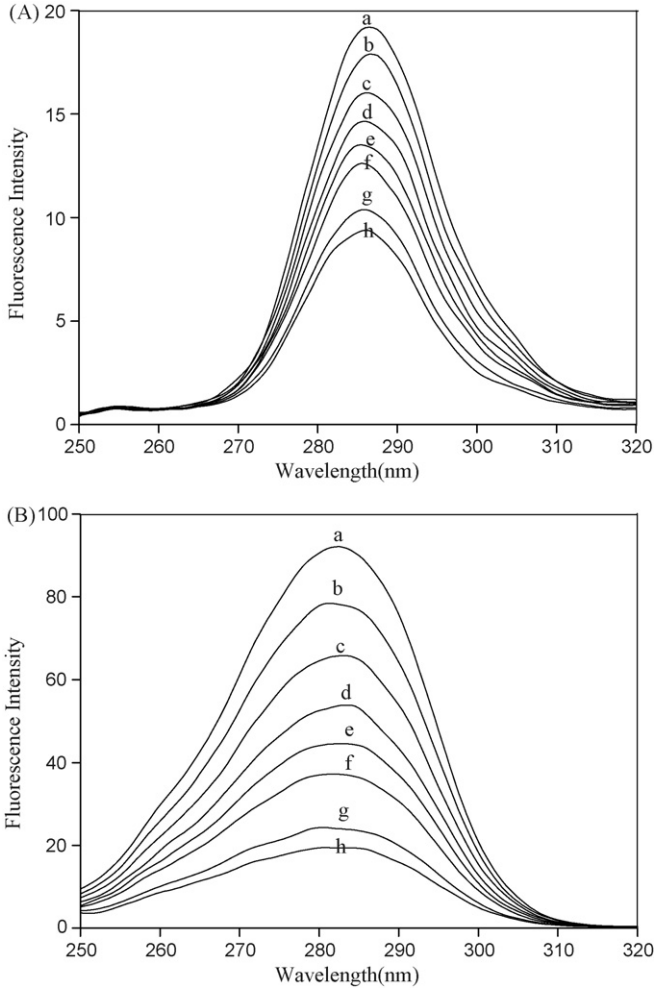

Fig. 5. Synchronous fluorescence spectra of HSA at pH 7.40 and 293 K. [HSA] = 3.5 μM; [farrerol] = 0 (a), 0.6 (b), 1.2 (c), 1.8 (d), 2.4 (e), 3.0 (f), 4.8 (g), and 6 μM (h). (A) $\Delta\lambda = 15$ nm and (B) $\Delta\lambda = 60$ nm.

farrerol are greater than the k_q of the scattered procedure show that the farrerol binding to HSA is quite strong and the quenching process belongs to a static quenching mechanism. As such, farrerol can be considered to be carried by HSA and removed together with HSA in body.

3.2. Conformational change of HSA by the interaction with farrerol

Fig. 5 illustrates synchronous fluorescence spectra of HSA with various amounts of farrerol recorded at $\Delta\lambda = 15$ nm (Fig. 5A) and $\Delta\lambda = 60$ nm (Fig. 5B), respectively. They are used for examination of the structural change of HSA upon addition of farrerol. As well known, synchronous fluorescence spectra can provide the information on the molecular microenvironment, particularly in the vicinity of the fluorophore functional groups. In our synchronous fluorescence experiments, the scanning interval $\Delta\lambda$ ($\Delta\lambda = \lambda_{emission} - \lambda_{excitation}$) was fixed at 15 and 60 nm, respectively. Thus, the experiment will provide the characteristic information for Try and Trp, respectively [24]. It can be seen that a little red shift of Trp fluorescence ($\lambda_{max} = 283$–285 nm in Fig. 5B) occurred with addition of farrerol, whereas the fluorescence band of Tyr shifted a little toward blue ($\lambda_{max} = 287$–285 nm in Fig. 5A). The former may represent the first indication that the conformation of HSA is somewhat changed, leading to the polarity around Trp residues strengthened and the hydrophobicity weakened [25]. The latter may suggest that the polarity around Tyr was decreased and the hydrophobicity increased [26].

Fig. 6 displays the CD spectra of HSA with various amounts of farrerol. They exhibit two negative ellipticities at 208 and 220 nm in far-UV region, which are characteristic of an α-helical structure of protein [27]. These observations imply the decreases in the α-helical content of a protein upon addition of farrerol. CD is a sensitive technique to monitor the conformational changes in proteins upon an interaction with a ligand. The interaction between farrerol and HSA causes a slight decrease in the band intensity at all wavelengths in the far-UV region without any significant shift of the peaks. Table 2 gives the results obtained from a quantitative analysis. The conformational change of HSA is confirmed by slight loss of its helical content, caused by the interaction with farrerol.

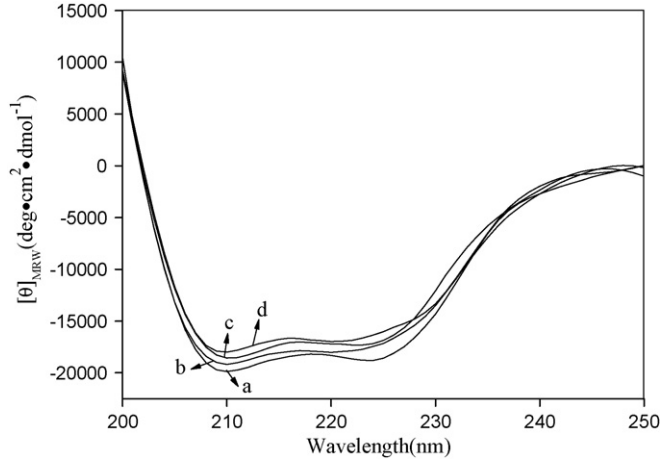

Fig. 6. CD spectra of HSA at 298 K and pH 7.40. [HSA] = 3.5 μM; [farrerol] = 0 (a), 6 (b), 18 (c), and 24 μM (d).

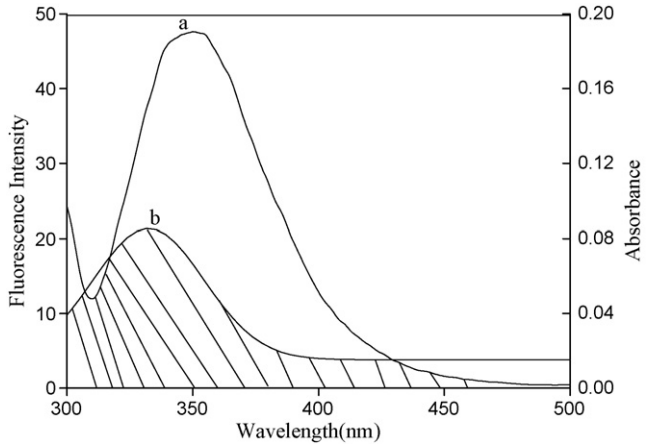

Fig. 7. Fluorescence emission spectrum of HSA (a) and absorption spectrum of farrerol (b) at [HSA] = [farrerol] = 3.5 μM.

3.3. Binding distance, mode, and site

Fig. 7 gives a fluorescence emission spectrum of pure HSA and an absorption UV–vis spectrum of pure farrerol. Since the fluorescence emission was affected by the excitation performed around 295 nm, the spectrum ranging from 300 to 500 nm was chosen to calculate the overlapping integral. From Eq. (7), where $F(\lambda)$ is the corrected fluorescence intensity of donor over a wavelength range of λ to $\lambda + \Delta\lambda$ and $\varepsilon(\lambda)$ the extinction coefficient of the acceptor at λ, and Fig. 7, J was calculated at 1.69×10^{-14} cm^3 L mol^{-1}. Consequently, $K^2 = 2/3$, $N = 1.36$, $\Phi = 0.14$ [28]. As such, R_0, E, and r were calculated at 2.72 nm, 0.55, and 2.63 nm, respectively. Obviously, the value for R_0 and r is much lower than 7 nm. This represents an indication that an interaction between the farrerol and HSA exists [29]. This result, in accord with requirements for Förster's theory, indicates there is no radiationless energy transfer between farrerol and HSA.

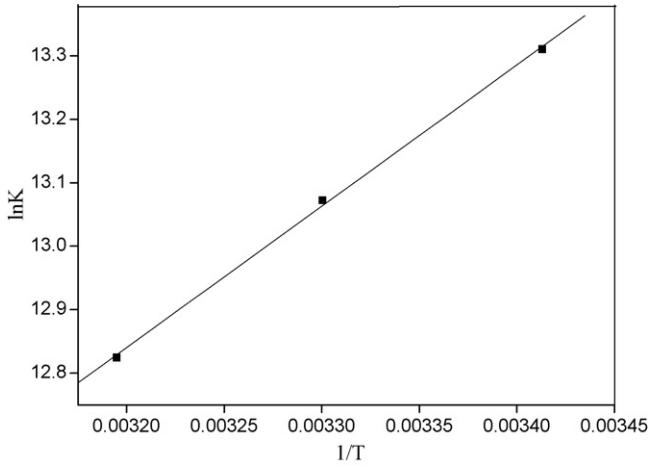

Fig. 8. Variation of ln K of the binding site with $1/T$.

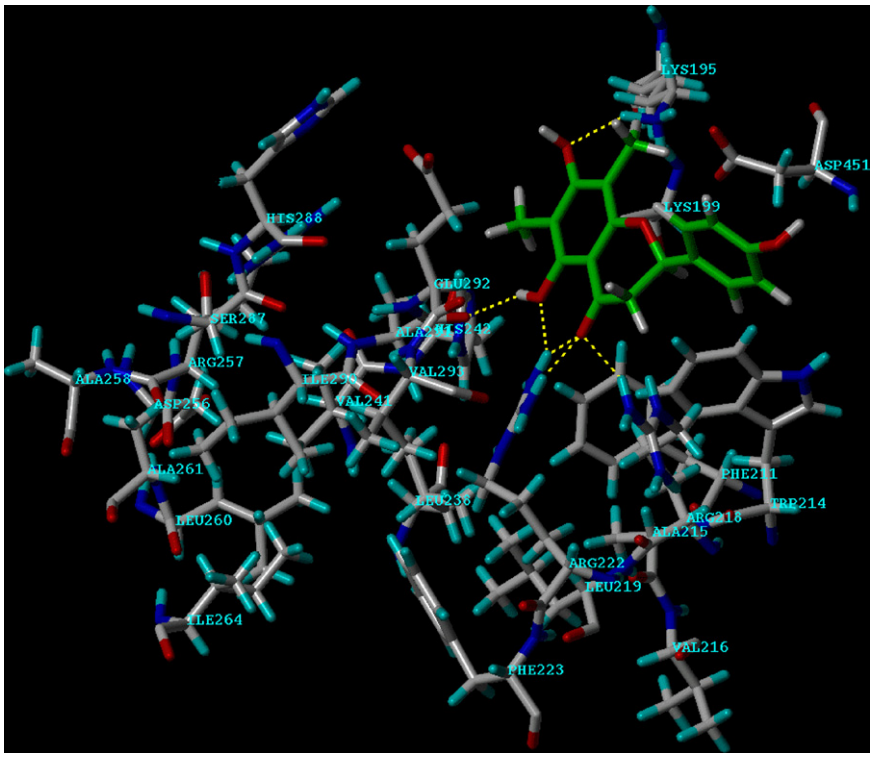

Fig. 9. Interaction modes between farrerol and HSA. Residues around 8 Å of the ligand are displayed only. The residues of HSA and the ligand structure are represented using ball and stick model. Hydrogen bonds between the ligand and the protein are represented using yellow dashed lines.

Table 1
Binding parameters for farrerol–HSA interaction at pH 7.40

T (K)	Stern–Volmer			Modified Scatchard		
	$K_{SV} \times 10^{-5}$ M^{-1}	$k_q \times 10^{-13}$ M^{-1} S^{-1}	r[a]	$K_A \times 10^{-5}$ M^{-1}	n	r[a]
293	5.02	5.02	0.998	6.03	0.48	0.999
303	4.02	4.02	0.998	4.76	0.46	0.999
313	3.09	3.09	0.999	3.71	0.50	0.997

[a] The regression coefficient.

Essentially, there are four types of non-covalent interaction existing in ligands binding to proteins: hydrogen bonds, van der Waals forces, hydrophobic bonds, and electrostatic interactions. In order to learn which interaction plays an important role in farrerol binding to HSA, the implication of the results presented above is discussed in conjunction with thermodynamic characteristics obtained for farrerol binding to HSA. Thermodynamic parameters were calculated from the van't Hoff plots (Fig. 8) and listed in Table 3. For a drug–protein interaction, a positive ΔS° is frequently taken as an evidence for a hydrophobic interaction [30] because water molecules are arranged in an ordered fashion around a ligand and proteins acquire more random configurations. A negative ΔH° value will be obtained whenever there exists a hydrogen bonding in the binding [31]. The negative ΔH° of -18.51 kJ mol^{-1} and positive ΔS° of 47.52 J mol^{-1} K^{-1}, therefore, show that both hydrogen bonds and hydrophobic interactions exist in the farrerol binding to HSA [32,33].

The experimental observations were followed up with molecular modeling studies, in which farrerol was assumedly docked to HSA for determining the preferred binding site on the protein. Based on a computational model building, the partial binding

Table 2
Effect of farrerol binding on the conformation of HSA

[Farrerol]/[HSA] molar ratio	θ_{Obs210} (mdeg)	$[\theta]_{MRW210}$ (deg cm^2 dmol^{-1})	α-Helical content (%)
0	−40.57	−19,872.5	54.7
1.70:1	−39.15	−19,173.4	52.3
5.10:1	−37.88	−18,553.2	50.2
6.80:1	−36.72	−17,986.8	48.2

Table 3
Thermodynamic parameters for farrerol–HSA interaction at pH 7.40

T (K)	ΔG° (kJ mol^{-1})	ΔH° (kJ mol^{-1})	ΔS° (J mol^{-1} K)
293	−32.43	−18.51	47.52
303	−32.91	−18.51	47.52
313	−33.38	−18.51	47.52

parameters of the farrerol–HSA system were calculated on a SGI O2 workstation. The best energy ranked results are shown in Fig. 9. It shows that farrerol is located at the site I within the binding pocket. It can be seen that the site I can accommodate a farrerol molecule. The farrerol moiety is located within the binding pocket and the A- and C-ring are practically coplanar. It is worth noting that Lys199 and Phe211 are in close proximity to the B-ring of farrerol, indicating the existence of hydrophobic contacts between them. But there exist also a number of hydrogen bonds between the 4-carbonyl oxygen of farrerol and Arg218 and Arg222 of HSA, 5-OH oxygen and Arg222, 5-OH hydrogen and Ala291, as well as 6-OH oxygen and Lys195. They will lead to a decrease in the hydrophilicity and an increase in the hydrophobicity of the farrerol–HSA system. As such, hydrophobic forces and hydrogen bond most likely play a major role in the binding of farrerol to HSA. These findings agree to the experimental observations.

4. Conclusions

The spectrophotometric observations and molecular modeling studies indicate that farrerol is bound to HSA and the bound residues of HSA include Lys195, Lys199, Phe211, Arg218, Arg222, and Ala291. The binding site is located at the site I in the hydrophobic pocket. A conformational change of HSA is caused by farrerol binding to HSA.

References

[1] E.L. Gelamo, C.H.T.P. Silva, H. Imasato, M. Tabak, Biochim. Biophys. Acta 1594 (2002) 84.
[2] I. Petitpas, T. Grüne, A.A. Bhattacharya, S. Curry, J. Mol. Biol. 314 (2001) 955.
[3] X.M. He, D.C. Carter, Nature 358 (1992) 209.
[4] T. Peters, Adv. Protein Chem. 37 (1985) 161.
[5] S. Curry, P. Brick, N.P. Frank, Biochim. Biophys. Acta 1441 (1999) 131.
[6] D.C. Carter, J.X. Ho, Adv. Protein Chem. 45 (1994) 153.
[7] T. Peters, All About Albumin. Biochemistry, Genetics and Medical Application, Academic Press, San Diego, 1996.
[8] C.D. Kanakis, P.A. Tarantilis, M.G. Polissiou, S. Diamantoglou, H.A. Tajmir-Riahi, J. Mol. Struct. 798 (2006) 69.
[9] J.N. Tian, J.Q. Liu, W.Y. He, Z.D. Hu, X.J. Yao, X.G. Chen, Biomacromolecules 5 (2004) 1956.
[10] W.Y. He, Y. Li, C.X. Xue, Z.D. Hu, X.G. Chen, F.L. Sheng, Bioorg. Med. Chem. 13 (2005) 1837.
[11] Y. Li, W.Y. He, Y.M. Dong, F.L. Sheng, Z.D. Hu, Bioorg. Med. Chem. 14 (2006) 1431.
[12] Y.H. Cao, C.G. Lou, Y.Z. Fang, J.N. Ye, J. Chromatogr. A 943 (2002) 153.
[13] P.B. Kandagal, S. Ashoka, J. Seetharamappa, V. Vani, S.M.T. Shaikh, J. Photochem. Photobiol. A 179 (2006) 161.
[14] A. Sharma, S.G. Schulman, Introduction of Fluorescence Spectroscopy, John Wiley & Sons Inc., New York, 1999, 58–59.
[15] J.R. Lakowica, G. Weber, Biochemistry 12 (1973) 4161.
[16] P.G. Yi, Q.S. Yu, Z.C. Shang, H.X. Zong, Acta Pharm. Sin. 35 (2000) 774.
[17] S.N. Timaseff, in: H. Peeters (Ed.), Proteins of Biological Fluids, Pergamon Press, Oxford, 1972, p. 511.
[18] L.A. Sklar, B.S. Hudson, R.D. Simoni, Biochemistry 16 (1977) 5100.
[19] I. Petitpas, A.A. Bhattacharya, S. Twine, M. East, S. Curry, J. Biol. Chem. 276 (2001) 22804.
[20] G. Morris, SYBYL Software, Version 6.9, Tripos Associates, St. Louis, 2002.
[21] J.R. Lakowicz, Principles of Fluorescence Spectroscopy, Plenum, New York, 1983, p. 265.
[22] A. Sulkowska, J. Mol. Struct. 614 (2002) 227.
[23] L. Trynda-Lemiesz, B.K. Keppler, H. Koztowski, J. Inorg. Biochem. 73 (1999) 123.
[24] J.H. Tang, F. Luan, X.G. Chen, Bioorg. Med. Chem. 14 (2006) 3210.
[25] B. Klajnert, M. Bryszewska, Bioelectrochemistry 55 (2002) 33.
[26] S.S. Lehrer, G.D. Fasman, J. Biol. Chem. 242 (1967) 4644.
[27] J.Q. Liu, J.N. Tian, W.Y. He, J.P. Xie, Z.D. Hu, X.G. Chen, J. Pharm. Biomed. Anal. 35 (2004) 671.
[28] L. Cyril, J.K. Earl, W.M. Sperry, Biochemists Handbook, E&FN Epon Led. Press, London, 1961, p. 83.
[29] W.Y. He, Y. Li, H.Z. Si, Y.M. Dong, F.L. Sheng, X.J. Yao, Z.D. Hu, J. Photochem. Photobiol. A 182 (2006) 158.
[30] J.N. Tian, J.Q. Liu, Z.D. Hu, X.G. Chen, Bioorg. Med. Chem. 13 (2005) 4124.
[31] P.D. Ross, S. Subramanian, Biochemistry 20 (1981) 3096.
[32] H. Aki, M. Yamamoto, J. Pharm. Pharmacol. 41 (1989) 674.
[33] N. Seedher, B. Singh, P. Singh, Indian J. Pharm. Sci. 51 (1999) 143.